Original Research Article

Unsteady MHD Flow of a Fluid past a Rotating Semi-Infinite Plate with Inclined Magnetic Field

ABSTRACT

This paper investigates unsteady two-dimensional MHD flow past a rotating semi-infinite plate with an inclined magnetic field with viscous dissipation, Ohmic and Joule heating. The fluid is assumed to be electrically conducting. The governing non-linear partial differential equations for mass, momentum, energy, concentration and magnetic field are transformed into a couple system by using appropriate dimensionless parameters and quantities. The coupled systems are then coded in MATLAB and solved simultaneously using the Gauss Seidel iteration technique. Various flow parameters and quantities are varied and their effects on velocity, temperature, and concentration profiles are investigated and discussed. It is observed that the transient velocity profiles increase with the increment of the Prandtl number, Grashof number, Hall parameter and Eckert number, while they decrease with the increase of the angle of inclination of the magnetic field and Hartman number. The temperature profiles rise with increasing the Grashof number, Hall parameter, Eckert number and Joule heating parameter while they decrease with increasing the Prandtl number, angle of inclination of magnetic field and Hartman number. The concentration profiles decline with increasing the Schmidt number and, the magnetic induction profiles decrease with increasing the magnetic Reynolds number and angle of inclination. The concept behind MHD is that the magnetic field induces current in a moving conductive fluid, which in turn generates a force on the fluid. This research is of great interest in applications such as MHD boats, pumps and magnetic material processing.

Keywords: MHD, Magnetic field, Velocity, temperature, Concentration.

1. INTRODUCTION

The magnetohydrodynamic (MHD) flow over a rotating plate has attracted a lot of attention due to its application in the manufacturing processes such as wire drawing, hot rolling, paper production, polymer extrusion, metal spinning and glass fibre [1]. A fluid that is electrically conducting and is subject to magnetic field is important because it can control the rate of cooling. Moreover, MHD flows have attracted a lot of attention in the field of engineering such as plasma studies, MHD generators, MHD pumps, accelerators and flow meters, geothermal energy extractions and nuclear reactors due to the effect of the magnetic field that is able to generate a force under an electrically conducting fluid [2, 3].

Most research studies in MHD have concentrated their focus on vertical, horizontal and inclined plates. Liu [4] in his research was able to investigate the effects of the magnetic field with mass and heat transfer over a stretching surface. Makinde [5] in his research investigated MHD heat and mass transfer over a plate that was vertically heated under convective boundary conditions. Many engineering and industrial applications and processes usually occur under high temperatures. The effect of heat absorption or generation in any fluid may alter the temperature distribution of the system [6].Thus, the knowledge of thermal effects in MHD is important in the usage and in the design process [7]. Moreover, the high temperatures during operations usually ionize the electrically conducting fluid during the heat transfer by radiation [8]. Thus, the knowledge of heat transfer becomes important in MHD research.

Seth et al. [9] in their research study were able to investigate MHD flow in presence of magnetic field past a rotating system that was inclined. The results of their study noted that the velocity of the fluid was accelerated by the angle of inclination. Kinyanjui et al. [10] investigated magnetohydrodynamic flow past a vertical plate that was rotating with effects of Hall current. They noted that the concentration, velocity and heat transfer of the fluid was affected by varying the magnetic field. The research study [11] on two dimension magneto-power-law mathematical model included the effects of Joule heating and viscous dissipation since they arise in in thermal magnetic polymeric process. Nandkeolyar et al. [12] on their numerical solutions of MHD unsteady fluid past a flat surface, noted that the species concentration of the fluid

increased with time but reduced with increase in Schmidt number. They also noted that the fluid temperature increased with the increase in the thermal diffusion. Seth et al. [13] in their research in MHD were able to obtain an exact solution for their research on an inclined magnetic field under the effects of hall current on a rotating vertical plate. The combined effects of thermal and mass diffusion for unsteady flow of an incompressible viscous fluid over a semi-infinite plate that was porous plate was also investigated by Ahmed et al. [14] and Eldabe et al. [15]. Their research demonstrated that thermal effects cannot be neglected in MHD flows. Sharma et al. [16] studied one dimensional flow past a vertical plate that was moving in the presence of the inclined magnetic field. Their research findings concluded that the velocity profiles were affected by varying different dimensionless parameters such as Prandtl number, Hartman number and Grashof number.

Prasad et al. [17] in their research of MHD flow investigated the effects of heat transfer of Hall current and magnetic field of an electrically conducting fluid with variable thickness over a stretching sheet. The governing equations that were non-linear were discretised using the explicit finite difference scheme. They noted that the Hall current and magnetic field had strong effects on the flow and heat transfer of the fluid. Maswai et al. [18] discretised the governing equations using the finite difference method on their research on turbulent MHD flow past a semi-infinite rotating plate with an inclined magnetic field. Iva et al. [19] investigated MHD free convection flow over a vertical plate with effects of heat source, hall current and suction. They noted that the species concentration, velocity and temperature of the fluid were dependent on the flow parameters that were varied. Ngesa et al. [20] investigated MHD mass and heat transfer past a porous semi-infinite plate. They concluded that the flow parameters had an influence on the fluid species concentration, velocity and temperature profiles. Moreover, the partial differential equations governing the flow were solved using the explicit difference method. The research study [21] on unsteady magnetohydrodynamic heat and mass transfer employed the explicit finite difference method to solve the non-linear differential equations and tested the stability and convergence of the method. Their research demonstrated that the finite difference method is a good numerical method to solve MHD problems. The research study [22, 23] also carried out stability and convergence analysis on the explicit finite difference scheme and noted that the numerical method was stable and was convergent. Bulinda et al. [24] studied free convection MHD flow of an incompressible fluid with effects of hall current, mass and heat transfer. Their research noted that velocity, species concentration and temperature of the fluid were affected by varying dimensionless numbers and parameters. They also concluded that thermal and hydrodynamic behaviours were important in MHD flows.

In spite of many studies in MHD, the unsteady convective flow past a semi-infinite rotating vertical plate in presence of an inclined magnetic field at an angle with effects of viscous dissipation, concentration and joule heating has yet to be researched extensively [30,31]. The non-linear MHD problem in this research is discretised using the finite difference method coupled with the Gauss iteration relaxation method. The effects of different parameters on momentum, species concentration and heat transfer characteristics are simulated and discussed in detail. Hence, the aim of the present study is to consider the effects of an inclined magnetic field taking into account the effects of viscous dissipation, concentration and joule heating. To the best of my knowledge, the proposed problem and results are new and have not been published before.

2. MATHEMATICAL ANALYSIS

The problem is a two-dimensional unsteady incompressible flow of an electrically conducting fluid past a rotating plate under the influence of magnetic field and heat transfer. The Hall current effect and the induced magnetic field are also considered. The Reynolds number is assumed to be small because the electric intensity is zero [25]. The plate is heated by convection with a hot fluid of temperature T_w. The geometry of the problem is given by Figure 1. The fluid is subjected to a magnetic field that is variable at an angle of α with the positive x axis in the xz plane. The system is made to rotate with uniform angular velocity in the presence of a magnetic field that is varied. The magnetic field that is applied is strong enough to generate the Hall current [8]. Induction effects are also generated to the sufficient magnitude of the magnetic Reynolds number.

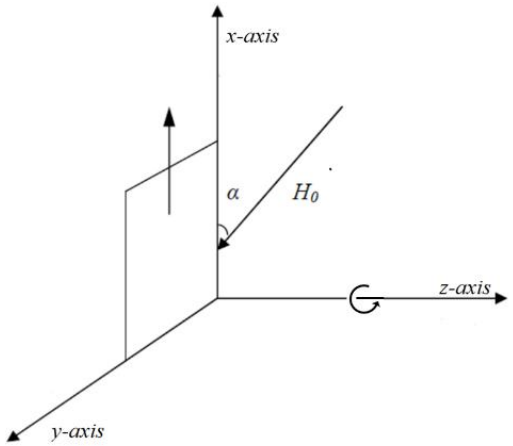

Fig. 1. Flow configuration and coordinate system.

The Ohm's law with effects of Hall current takes the form of [26],

$$\hat{J} + \frac{\omega_e \tau_e}{H_0}\left[\hat{J} \times \hat{H}\right] = \sigma\left[\hat{E} + \mu_e \hat{q} \times \hat{H} + \frac{1}{en_e}\nabla \cdot p_e\right] \tag{1}$$

Neglecting the applied electric field and the electron pressure gradient, equation (1) reduces to

$$\hat{J} + \frac{\omega_e \tau_e}{H_0}\left[\hat{J} \times \hat{H}\right] = \sigma\left[\mu_e \hat{q} \times \hat{H}\right] \tag{2}$$

Considering the vector quantities equations,

$q = (u, v, 0)$, $H = (H_x + H_0 \cos\alpha, 0, H_z + H_0 \sin\alpha)$, $J = (J_x, J_y, J_z)$

According to the research [27], the current density components in x and y direction considering that J_z is zero are given by,

$$J_x = \frac{\sigma\mu_e H_0 (H_z + H_0 cos\alpha)(m(H_z + H_0 sin\alpha)u + H_0 v)}{H_0^2 + m^2(H_z + H_0 sin\alpha)^2} \tag{3}$$

$$J_y = \frac{\sigma\mu_e H_0 (H_z + H_0 sin\alpha)(m(H_z + H_0 sin\alpha)v - H_0 u)}{H_0^2 + m^2(H_z + H_0 sin\alpha)^2} \tag{4}$$

Assuming that $\frac{\partial w}{\partial z} = 0$, Partially integrating this equation in terms of z, we obtain $w = -u_0$ which represents a constant injection in the negative x direction. The continuity, momentum, energy, concentration and magnetic field equations under Boussinesq boundary layer approximations are given by, [28]

$$\frac{\partial u}{\partial x} + \frac{\partial w}{\partial z} = 0 \tag{5}$$

$$\begin{aligned} &\frac{\partial u}{\partial t} + u\frac{\partial u}{\partial x} - u_0\frac{\partial u}{\partial z} + 2\Omega v \\ &\quad = g\beta(T - T_\infty) + \vartheta\left(\frac{\partial^2 u}{\partial x^2} + \frac{\partial^2 u}{\partial z^2}\right) + \beta g(C - C_\infty) \\ &\quad + \frac{\sigma\mu_e H_0 (H_z + H_0 sin\alpha)(m(H_z + H_0 sin\alpha)v - H_0 u)}{\rho(H_0^2 + m^2(H_z + H_0 sin\alpha)^2)} \end{aligned} \tag{6}$$

$$\frac{\partial v}{\partial t}+u\frac{\partial v}{\partial x}-u_0\frac{\partial v}{\partial z}+2\Omega u=\vartheta\left(\frac{\partial^2 v}{\partial x^2}+\frac{\partial^2 v}{\partial z^2}\right)+\frac{\sigma\mu_e H_0(H_z+H_0 sin\alpha)(m(H_z+H_0 sin\alpha)u+H_0 v)}{\rho(H_0^2+m^2(H_z+H_0 sin\alpha)^2)} \quad (7)$$

$$\rho C_p\left[\frac{\partial T}{\partial t}+u\frac{\partial T}{\partial x}+u_0\frac{\partial T}{\partial z}\right]=k\left[\frac{\partial^2 T}{\partial x^2}+\frac{\partial^2 T}{\partial z^2}\right]+\vartheta\left[\left(\frac{\partial u}{\partial z}\right)^2+\left(\frac{\partial v}{\partial z}\right)^2\right]+\sigma{\mu_e}^2(H_z+H_0 sin\alpha)^2(u^2+v^2) \quad (8)$$

$$\frac{\partial C}{\partial t}+u\frac{\partial C}{\partial x}+u_0\frac{\partial C}{\partial z}=D\left(\frac{\partial^2 C}{\partial x^2}+\frac{\partial^2 C}{\partial z^2}\right) \quad (9)$$

$$\frac{\partial H_x}{\partial t}=H_0 sin\alpha\frac{\partial u}{\partial z}+\frac{\partial}{\partial z}(uH_x)+\frac{1}{\sigma\mu_e}\left(\frac{\partial^2 H_x}{\partial x^2}+\frac{\partial^2 H_x}{\partial z^2}\right) \quad (10)$$

$$\frac{\partial H_z}{\partial t}=H_0 sin\alpha\frac{\partial u}{\partial z}-\frac{\partial}{\partial x}(uH_z)+\frac{1}{\sigma\mu_e}\left(\frac{\partial^2 H_z}{\partial x^2}+\frac{\partial^2 H_z}{\partial z^2}\right) \quad (11)$$

The initial and boundary conditions for the MHD problem are given by,

$$\begin{aligned}&t=0,\quad u(x,z,t)=0,\ v(x,z,t)=0,\ T(x,z,t)=T_\infty,\ C(x,z,t)=C_\infty,\ H(x,z,t)=0\\&t>0,\quad u(0,z,t)=0,\ v(0,z,t)=0,T(0,z,t)=T_w,\ C(x,z,t)=C_w,\ H(0,z,t)=H_0\\&t>0,\quad u(\infty,z,t)=0,v(\infty,z,t)=0,T(\infty,z,t)=T_\infty,C(\infty,z,t)=C_\infty,H(\infty,z,t)=H_0\end{aligned} \quad (12)$$

The following dimensionless quantities and variables are introduced into the continuity, momentum, concentration and energy balance equations; that is,

$$\begin{aligned}&\bar{x}=\frac{x\,u_0}{u},\quad \bar{z}=\frac{z\,u_0}{u},\quad \bar{t}=\frac{t\,u_0^2}{u},\quad \bar{u}=\frac{u}{u_0},\quad \bar{v}=\frac{v}{u_0}\\&\bar{H}_x=\frac{H_x}{H_0},\quad \bar{H}_z=\frac{H_z}{H_0},\quad \theta=\frac{T-T_\infty}{T_w-T_\infty},\quad P_r=\frac{\mu_e C_p}{k},\quad R=\frac{H_0\sigma}{\rho C_p}\\&G_r=\frac{g\beta\theta\vartheta(T_w-T_\infty)}{u_0^3},\quad M^2=\frac{\sigma\mu_e H_0^2\vartheta}{u_0^2\rho},\quad G_c\frac{g\beta\vartheta(C-C_\infty)}{u_0^3}\\&R_m=\mu_e u_0\sigma,\quad E_r=\frac{\Omega\vartheta}{u_0^2},\quad S_c=\frac{D}{\vartheta},\quad E_c=\frac{u_0^3}{(T_w-T_\infty)\,C_p},\quad \bar{C}=\frac{C-C_\infty}{C_w-C_\infty}\end{aligned} \quad (13)$$

and we obtain

$$\frac{\partial\bar{u}}{\partial\bar{x}}+\frac{\partial\bar{v}}{\partial\bar{z}}=0 \quad (14)$$

$$\frac{\partial\bar{u}}{\partial\bar{t}}-u_0\frac{\partial\bar{u}}{\partial\bar{z}}+\bar{u}\frac{\partial\bar{u}}{\partial\bar{x}}-2E_r\bar{v}=\theta G_r+\left(\frac{\partial^2\bar{u}}{\partial\bar{x}^2}+\frac{\partial^2\bar{u}}{\partial\bar{z}^2}\right)+G_c\bar{C}+M^2(\bar{H}_x+sin\alpha)^2\left(\frac{m(H_z+sin\alpha)\bar{v}-\bar{u}}{1+m^2(\bar{H}_z+sin\alpha)^2}\right) \quad (15)$$

$$\frac{\partial\bar{v}}{\partial\bar{t}}-u_0\frac{\partial\bar{v}}{\partial\bar{z}}+\bar{u}\frac{\partial\bar{v}}{\partial\bar{x}}+2E_r\bar{u}=\left(\frac{\partial^2\bar{v}}{\partial\bar{x}^2}+\frac{\partial^2\bar{v}}{\partial\bar{z}^2}\right)-M^2(\bar{H}_z+sin\alpha)^2\left(\frac{m(H_z+sin\alpha)\bar{v}+\bar{u}}{1+m^2(\bar{H}_z+sin\alpha)^2}\right) \quad (16)$$

$$\frac{\partial\theta}{\partial\bar{t}}+\bar{u}\frac{\partial\theta}{\partial\bar{x}}+u_0\frac{\partial\theta}{\partial\bar{z}}=\frac{1}{P_r}\left[\frac{\partial^2\theta}{\partial\bar{x}^2}+\frac{\partial^2\theta}{\partial\bar{z}^2}\right]+E_c\left[\left(\frac{\partial\bar{u}}{\partial\bar{z}}\right)^2+\left(\frac{\partial\bar{v}}{\partial\bar{z}}\right)^2\right]+R(\bar{H}_z+sin\alpha)^2(\bar{u}^2+\bar{v}^2) \quad (17)$$

$$\frac{\partial \bar{C}}{\partial \bar{t}} + \frac{\partial \bar{C}}{\partial \bar{x}} + \frac{\partial \bar{C}}{\partial \bar{z}} = S_c\left(\frac{\partial^2 \bar{C}}{\partial \bar{x}^2} + \frac{\partial^2 \bar{C}}{\partial \bar{z}^2}\right) \tag{18}$$

$$\frac{\partial \bar{H}_x}{\partial \bar{t}} = sin\alpha \frac{\partial \bar{u}}{\partial \bar{z}} + \frac{\partial}{\partial \bar{z}}(\bar{u}\bar{H}_z) + \frac{1}{R_m}\left(\frac{\partial^2 \bar{H}_x}{\partial \bar{x}^2} + \frac{\partial^2 \bar{H}_x}{\partial \bar{z}^2}\right) \tag{19}$$

$$\frac{\partial \bar{H}_z}{\partial \bar{t}} = sin\alpha \frac{\partial \bar{u}}{\partial \bar{z}} - \frac{\partial}{\partial \bar{x}}(\bar{u}\bar{H}_z) + \frac{1}{R_m}\left(\frac{\partial^2 \bar{H}_z}{\partial \bar{x}^2} + \frac{\partial^2 \bar{H}_z}{\partial \bar{z}^2}\right) \tag{20}$$

With dimensionless initial and boundary conditions,

$$\begin{aligned}
&\bar{t} = 0, \quad \bar{u}(\bar{x},\bar{z},\bar{t}) = 0,\ \bar{v}(\bar{x},\bar{z},\bar{t}) = 0, \theta(\bar{x},\bar{z},\bar{t}) = 0,\ \bar{C}(\bar{x},\bar{z},\bar{t}) = 0, H(x,\bar{z},\bar{t}) = 0\\
&\bar{t} > 0, \quad \bar{u}(x,\bar{z},\bar{t}) = 1,\ \bar{v}(0,\bar{z},\bar{t}) = 0,\ \theta(0,\bar{z},\bar{t}) = 1,\ \bar{C}(\bar{x},\bar{z},\bar{t}) = 1, H(0,\bar{z},\bar{t}) = 1\\
&\bar{t} > 0, \quad \bar{u}(\infty,\bar{z},\bar{t}) = 0,\ \bar{v}(\infty,\bar{z},\bar{t}) = 0,\ \theta(\infty,\bar{z},\bar{t}) = 0,\ \bar{C}(\infty,\bar{z},\bar{t}) = 0, H(\infty,\bar{z},\bar{t}) = 0
\end{aligned} \tag{21}$$

3. NUMERICAL PROCEDURE

The finite difference method is used to discretise the governing equations together with their initial and boundary conditions. The discretization is usually based on a linear mesh and uniform grid on the Cartesian plane. Firstly, a spatial interval $0 \le dx \le n_{max}$ partition is introduced in the x and z axis. This partition is then subdivided into N equal parts with grid sizes $d\bar{x} = d\bar{z} = d\bar{t} = 1/N$ and $d\bar{z} = 1/N$ and grid points $\bar{x}_i = (i-1)dx, 1 \le i \le N+1$, $\bar{z}_i = (j-1)d\bar{z}, 1 \le j \le N+1$ and $\bar{t}_i = (k-1)d\bar{t}, 1 \le k \le N+1$.

The first and second order spatial derivatives are approximated with central finite differences. The discrete system for the MHD problem becomes

$$\begin{aligned}
\bar{u}_{i,j}^k = \left(\frac{M^2(\bar{H}_z + sin\,\alpha)^2}{1 + m^2(\bar{H}_z + sin\alpha)^2} + \frac{2}{(d\bar{x})^2} + \frac{2}{(d\bar{z})^2}\right)^{-1} \Bigg[& \frac{-1}{2d\bar{x}}\left(\left(\bar{u}_{i+1,j}^k\right)^2 - \left(\bar{u}_{i-1,j}^k\right)^2\right)\\
& + \frac{1}{(d\bar{x})^2}\left(\bar{u}_{i+1,j}^k - \bar{u}_{i-1,j}^k\right) - \frac{u_0}{2d\bar{z}}\left(\bar{u}_{i,j+1}^k - \bar{u}_{i,j-1}^k\right) + \frac{1}{(d\bar{z})^2}\left(\bar{u}_{i,j+1}^k - \bar{u}_{i,j-1}^k\right) - 2E_r\bar{u}_{i,j}^k\\
& - M^2(\bar{H}_z + sin\alpha)^2\left(\frac{m(\bar{H}_z sin\alpha)\bar{u}_{i,j}^k}{1 + m^2(\bar{H}_z + sin\alpha)^2}\right)\Bigg]
\end{aligned} \tag{22}$$

$$\begin{aligned}
\bar{v}_{i,j}^k = \left(\frac{M^2(\bar{H}_z + sin\alpha)^2}{1 + m^2(\bar{H}_z + sin\alpha)^2} + \frac{2}{(d\bar{x})^2} + \frac{2}{(d\bar{z})^2}\right)^{-1} \Bigg[& \frac{-1}{2d\bar{x}}\left(\bar{v}_{i+1,j}^k\bar{u}_{i+1,j}^k - \bar{v}_{i-1,j}^k\bar{u}_{i-1,j}^k\right)\\
& + \frac{1}{(d\bar{x})^2}\left(\bar{v}_{i+1,j}^k - \bar{v}_{i+1,j}^k\right) - \frac{u_0}{2d\bar{z}}\left(\bar{v}_{i,j+1}^k - \bar{v}_{i,j-1}^k\right) + \frac{1}{(d\bar{z})^2}\left(\bar{v}_{i,j+1}^k - \bar{v}_{i,j-1}^k\right) + \theta G_r\\
& + 2E_r\bar{v}_{i,j}^k + M^2(\bar{H}_z + sin\alpha)^2\left(\frac{m(\bar{H}_z + sin\alpha)\bar{v}_{i,j}^k}{1 + m^2(\bar{H}_z + sin\alpha)^2}\right)\Bigg]
\end{aligned} \tag{23}$$

$$\begin{aligned}
\theta_{i,j}^k = \left[\frac{P_r(d\bar{x})^2(d\bar{z})^2}{2(d\bar{x})^2 + 2(d\bar{z})^2}\right] \Bigg[& \frac{-1}{2d\bar{x}}\left(\theta_{i+1,j}^k\bar{u}_{i+1,j}^k - \theta_{i-1,j}^k\bar{u}_{i-1,j}^k\right) - \frac{u_0}{2d\bar{z}}\left(\theta_{i,j+1}^k - \theta_{i,j-1}^k\right)\\
& + \frac{E_c}{4}\left(\frac{(\bar{u}_{i+1,}^k + \bar{u}_{i-1,j}^k)^2}{(d\bar{x})^2} + \frac{(\bar{v}_{i,j+1}^k + \bar{v}_{i,j-1}^k)^2}{(d\bar{z})^2}\right) + \frac{1}{P_r}\left(\frac{\theta_{i+1,j}^k + \theta_{i-1,j}^k}{(d\bar{x})^2} + \frac{\theta_{i,j+1}^k + \theta_{i,j-1}^k}{(d\bar{z})^2}\right)\\
& + R(\bar{H}_z + sin\alpha)^2((\bar{u}_{i,j}^k)^2 + (\bar{v}_{i,j}^k)^2)\Bigg]
\end{aligned} \tag{24}$$

$$\bar{C}_{i,j}^{k}=\left[\frac{S_c}{(d\bar{x})^2}+\frac{S_c}{(d\bar{z})^2}-\frac{1}{d\bar{t}}\right]^{-1}\left[-\left(\frac{\bar{C}_{i,j+1}^{k}-\bar{C}_{i,j-1}^{k}}{2d\bar{x}}\right)-\left(\frac{\bar{C}_{i,j+1}^{k}-\bar{C}_{i,j-1}^{k}}{2d\bar{z}}\right)+S_c\left(\frac{\bar{C}_{i+1,j}^{k}+\bar{C}_{i+1,j}^{k}}{(d\bar{x})^2}+\frac{\bar{C}_{i,j-1}^{k}+\bar{C}_{i,j-1}^{k}}{(d\bar{z})^2}\right)-\frac{\bar{C}_{i,j}^{k+1}}{d\bar{t}}\right] \tag{25}$$

$$(\bar{H}_x)_{i,j}^{k}=\left[\frac{1}{R_m(d\bar{x})^2}+\frac{1}{R_m(d\bar{z})^2}-\frac{1}{d\bar{t}}\right]^{-1}\left[-sin\alpha\left(\frac{\bar{u}_{i,j+1}^{k}-\bar{u}_{i,j-1}^{k}}{2d\bar{z}}\right)+\left(\frac{\bar{u}_{i,j+1}^{k}(\bar{H}_x)_{i,j+1}^{k}-\bar{u}_{i,j-1}^{k}(\bar{H}_x)_{i,j-1}^{k}}{2d\bar{z}}\right)+\frac{1}{2R_m}\left(\frac{(\bar{H}_x)_{i+1,j}^{k}+(\bar{H}_x)_{i+1,j}^{k}}{(d\bar{x})^2}+\frac{(\bar{H}_x)_{i,j-1}^{k}+(\bar{H}_x)_{i,j-1}^{k}}{(d\bar{z})^2}\right)-\frac{(\bar{H}_x)_{i,j}^{k+1}}{d\bar{t}}\right] \tag{26}$$

$$(\bar{H}_z)_{i,j}^{k}=\left[\frac{1}{R_m(d\bar{x})^2}+\frac{1}{R_m(d\bar{z})^2}-\frac{1}{d\bar{t}}\right]^{-1}\left[sin\alpha\left(\frac{\bar{u}_{i,j+1}^{k}-\bar{u}_{i,j-1}^{k}}{2d\bar{z}}\right)+\left(\frac{\bar{u}_{i,j+1}^{k}(\bar{H}_z)_{i,j+1}^{k}-\bar{u}_{i,j-1}^{k}(\bar{H}_z)_{i,j-1}^{k}}{2d\bar{z}}\right)+\frac{1}{2R_m}\left(\frac{(\bar{H}_z)_{i+1,j}^{k}+(\bar{H}_z)_{i+1,j}^{k}}{(d\bar{x})^2}+\frac{(\bar{H}_z)_{i,j-1}^{k}+(\bar{H}_z)_{i,j-1}^{k}}{(d\bar{z})^2}\right)-\frac{(\bar{H}_z)_{i,j}^{k+1}}{d\bar{t}}\right] \tag{27}$$

4. RESULTS AND DISCUSSION

The approximation solutions for the MHD problem are obtained for various parameters. In order to analyse the unsteady state model, various numerical values of the non-dimensional velocity, temperature and concentration have been computed for different values of Prandtl number, Grashof number, inclination angle, Hall parameter, Eckert number, Hartman number, Joule heating parameter, magnetic Reynolds number and Schmidt number.

4.1 Effects of parameter variation on velocity profiles

Figures 2-7 demonstrate the effects of various parameters on the velocity profiles. It is observed from Figure 2 that increasing the Prandtl number leads to a decrease in the velocity of the flow field. The Prandtl number is a ratio of the kinematic viscosity to thermal diffusivity of the fluid. Thus, an increase in Prandtl number results to an increase in the kinematic viscosity, which results to the fluid becoming more viscous, and in turn leads to a decrease in the velocity of the flow field. The effects of Grashof number are presented in Figure 3. The Grashof number is the ratio of the thermal buoyancy force to viscous hydrodynamic force in the flow of the boundary layer. It is noted that the transient velocity increases with increasing the Grashof number. The buoyancy force enhances the gravitational force, which increases the velocity profiles. The velocity increases reaching a peak value near the surface of the plate and then decreases to zero, satisfying the far field condition. This is due to increase in the thermal buoyance force. Figure 4 represents the effects of angle of inclination of the magnetic field on the transient velocity profiles. It is observed that the transient velocity profiles decrease with increasing the angle of inclination. This is due to reduction in the magnetic field, which increases the Lorenz force. This force leads to resistance due to greater drag that is experienced at the plate surface, thereby reducing the flow motion of the fluid. Figure 5 demonstrates the effects of Hall parameter on the transient velocity profiles of the fluid. It is observed that the transient velocity profiles increase with increasing the Hall parameter. An increase in the Hall parameter leads to a decrease in the effective conductivity, which reduces the magnetic damping force. This reduction in the magnetic damping force increases the velocity of the fluid. Figure 6 depicts the effects of Eckert number on the transient velocity profiles. An increase in Eckert number results in an increase in the viscous heating of the fluid. This makes the fluid lighter and hence flow faster. The different values of the Hartman number for the velocity profiles are illustrated in Figure 7. The velocity decreases with increasing the Hartman number due to increase in the Lorentz force that is generated by the magnetic field. This force opposes the fluid flow, leading to a decrease in the momentum of the fluid. The transient velocity profiles analysis and nature when different parameters are varied are in good agreement with earlier results as researched by Adem [29].

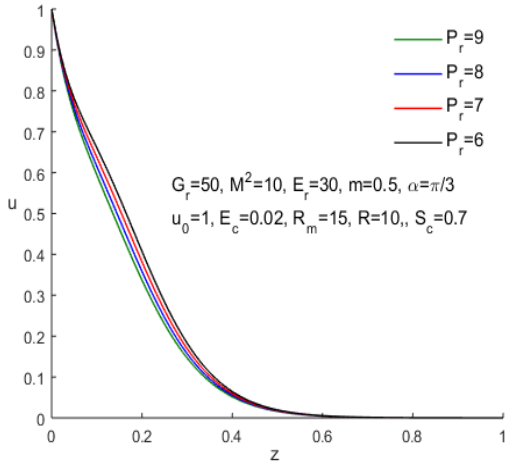

Fig. 2. Velocity profiles for various values of P_r.

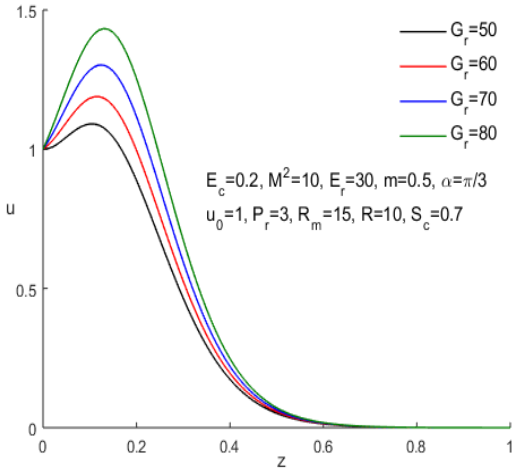

Fig. 3. Velocity profiles for various values of G_r.

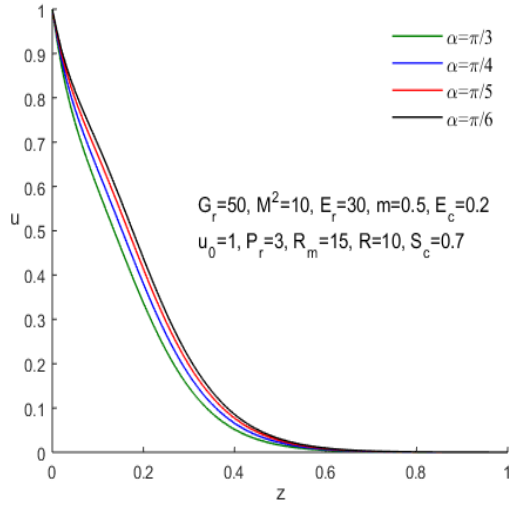

Fig. 4. Velocity profiles for various values of angle α.

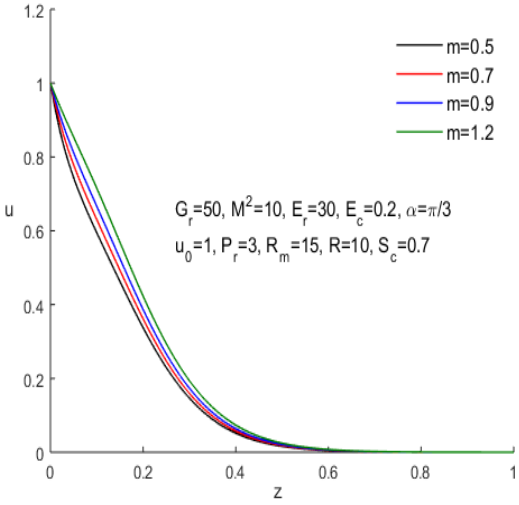

Fig. 5. Velocity profiles for various values of m.

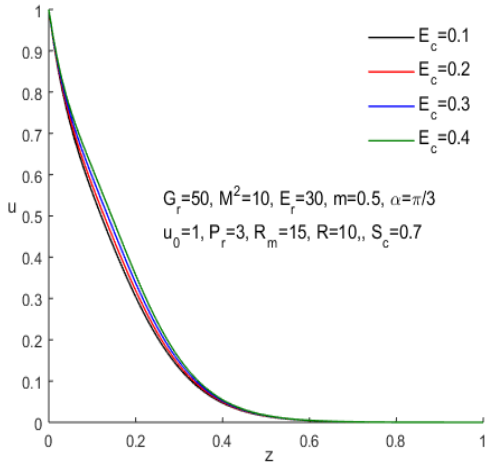

Fig. 6. Velocity profiles for various values of E_c.

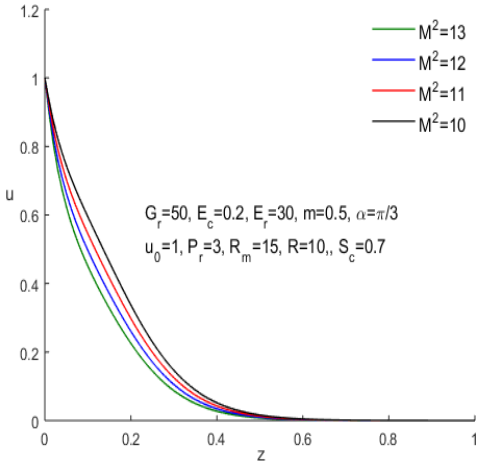

Fig. 7. Velocity profiles for various values of M^2.

4.2 Effects of parameter variation on temperature profiles

Figures 8-14 illustrate the temperature profiles for different parameters variations. It is observed from all these figures that the temperature increases, reaching the peak near the surface of the plate and then decreases to zero (free stream value) satisfying the boundary conditions. The temperature of the fluid is reduced when the Prandtl number is increased, as illustrated in Figure 8. The thermal conductivity of the fluid increases with a decrease in the Prandtl number. This makes heat diffuse away from the surface that is heated more rapidly, which distributes the heat and contributes to a higher fluid temperature. These findings on effect of Prandtl number on temperature profiles coincide with the research study [28]. Figure 9 illustrates the effects of Grashof number on the fluid temperature. Increasing the Grashof number results in an increase in the thermal buoyancy force, which makes heat to be conducted from the plate into the fluid, increasing the temperature of the fluid. Figure 10 illustrates the effects of the inclination angle on the fluid temperature. Increasing the magnetic inclination angle results in a reduction in the fluid temperature. Increasing the angle of inclination results in a reduction in the rate of heat transfer. This is as a result of thickening of the thermal boundary layer, which reduces the rate of heat transfer, thus a reduction in fluid temperature. Figure 11 illustrates the effects of Hall parameter on the temperature profiles. It is observed that the temperature of the fluid increases with increase in the Hall parameter. The thermal boundary layer thickening decreases as a result of increase in Hall parameter. This means the temperature gradient reduces, which in turn increases the fluid temperature. Figure 12 illustrates that the temperature of the fluid increases with increase in Eckert number. The Eckert number expresses the contribution of the kinetic energy in the flow and the difference in enthalpy in the boundary layer. The cooling of the wall is aided by positive Eckert number and therefore aiding heat transfer to the fluid. Increasing the Eckert number results in viscous heating due to frictional drag force, which constitutes additional internal heat generation, resulting in elevation of the temperature of the fluid. The temperature of the fluid reduces with increase in Hartman number, as illustrated in Figure 13. The Lorenz force reduces the thermal viscous dissipation in the fluid, resulting in a thinner boundary layer. Figure 14 illustrates the effects of Joule heating parameter on the temperature profiles. An increase in the Joule heating parameter results in an increase in the temperature of the fluid. An increase in the Joule heating Parameter means more current on the plate, which in turn leads to more heating of the fluid, thereby increasing its temperature. The temperature profiles analysis and nature when different parameters are varied are in good agreement with earlier results as researched by Adem [29].

4.3 Effects of parameter variation on concentration profile

Figure 15 shows that the species concentration decreases with increase in Schmidt number. The Schmidt number is the ratio of the viscosity of the fluid to the mass diffusivity. An increase in the Schmidt number implies a decrease in the mass diffusivity rate of the fluid. This reduces the concentration of boundary layer, which leads to an overall reduction in the species concentration. The concentration profiles nature and analysis when different parameters are varied are in good agreement with earlier results as reported by Adem [29].

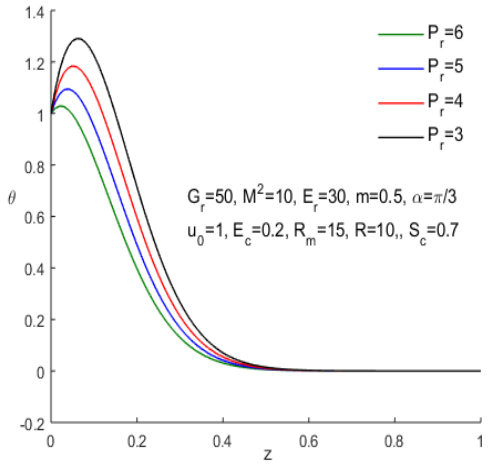

Fig. 8. Temperature profiles for various values of P_r.

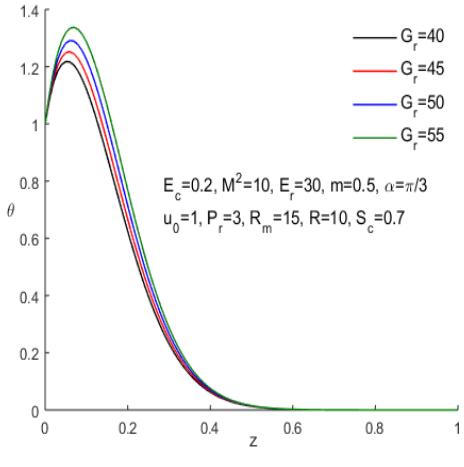

Fig. 9. Temperature profiles for various values of G_r.

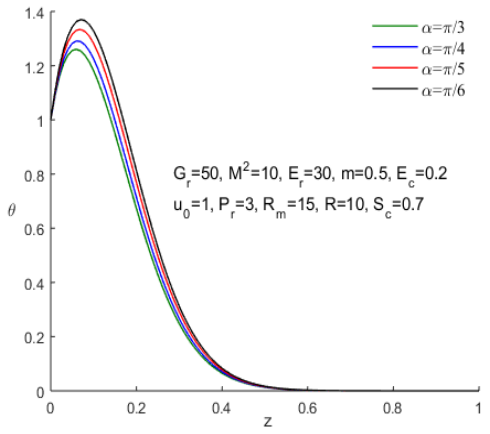

Fig. 10. Temperature profiles for various values of α.

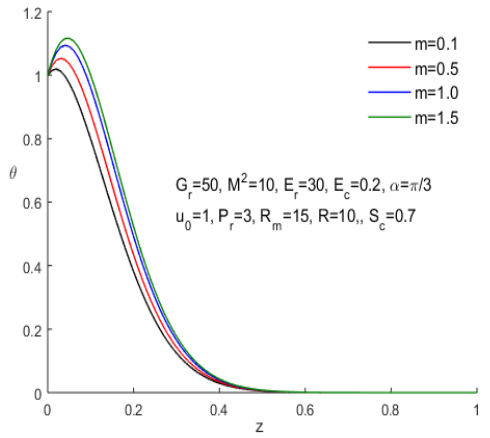

Fig. 11. Temperature profiles for various values of m.

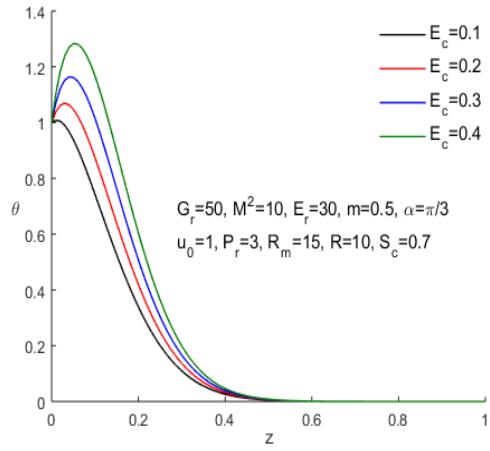

Fig. 12. Temperature profiles for various values of $\mathrm{E_c}$.

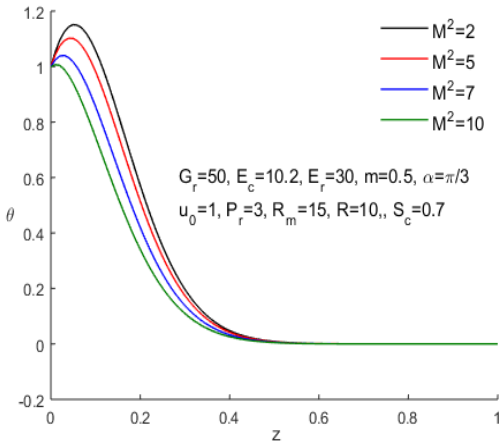

Fig. 13. Temperature profiles for various values of $\mathrm{M^2}$.

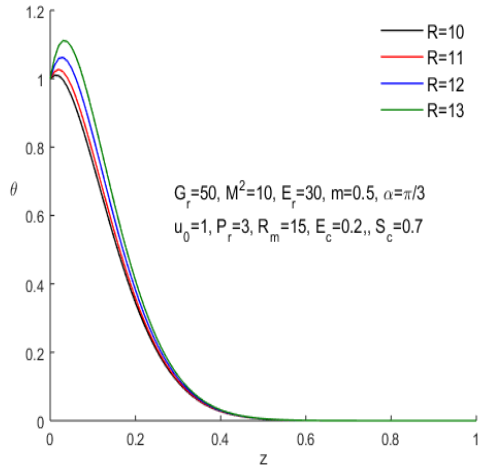

Fig 14. Temperature profiles for various values of R.

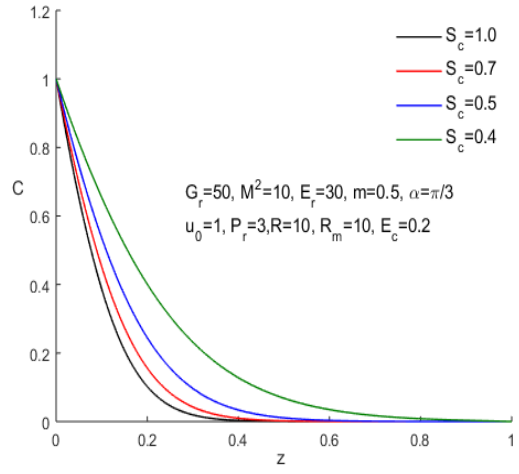

Fig 15. Concentration profiles for various values of S_c.

4.4 Effects of parameter variation on magnetic induction profiles

Figure 16 illustrates the effect of magnetic Reynolds number on magnetic induction profiles. It is noted that the magnetic induction reduces with increasing the magnetic Reynolds number. The magnetic Reynolds number is a ratio of the fluid flux to the mass diffusivity. Thus, increasing the magnetic Reynolds number means a reduction in the mass diffusivity. The reduction in the mass diffusivity disrupts the diffusion of the magnetic fields, which leads to a decline in the magnetic field. Figure 17 illustrates that the magnetic induction reduces with increasing the angle of inclination. An increase in the angle reduces the electromotive force, which in turn reduces the magnetic induction. The magnetic induction profiles nature and analysis when different parameters are varied, are in good agreement with earlier results as researched by Muthiga et al. [27].

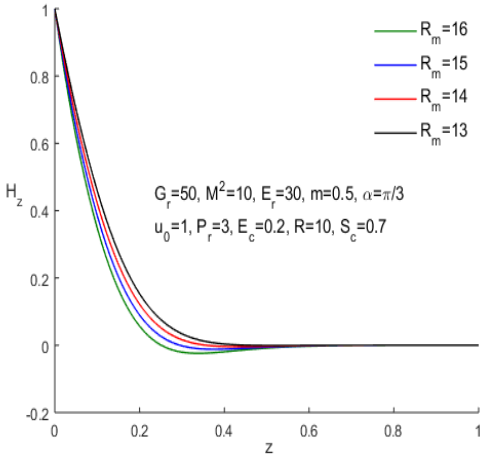

Fig 16. Magnetic induction profiles for various values of $\mathbf{R_m}$.

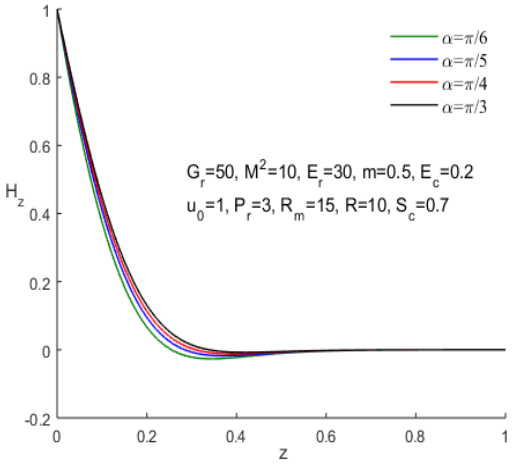

Fig 17. Magnetic induction profiles for various values of α.

4. CONCLUSIONS

A numerical analysis is investigated for the study of the unsteady MHD flow of fluid past a rotating semi-infinite vertical plate with the inclined magnetic field. The non-linear model problem is solved numerically using the finite difference method coupled with the Gauss Seidel iteration technique. The key findings from the research are given below:

(i) The transient velocity profiles increase with increase in Prandtl number, Grashof number, Hall parameter and Eckert number. However, they decline with increment in the angle of inclination of the magnetic field and Hartman number.

(ii) The temperature profiles increase with increase in the Grashof number, Hall parameter, Eckert number and Joule heating parameter. However, they decline with increment in the Prandtl number, angle of inclination of magnetic field and Hartman number.

(iii) Increasing the Schmidt number tends to diminish the concentration profiles.

(iv) The magnetic induction profiles decrease with increment in the magnetic Reynolds number and angle of inclination.

Nomenclature

C Concentration of species (mol m^{-3})
$\bar{C}$ Dimensionless concentration of species
C_w Concentration of species at plate (mol m^{-3})
C_∞ Concentration of species at free stream (mol m^{-3})
C_p Specific heat constant pressure (J . kg^{-1}. K^{-1})
D Diffusion coefficient (m^2 s^{-1})
e Electric charge (C)
E Electric field (kg m s^{-2} C^{-1})
E_c Eckert number
E_r Rotation parameter
G_c Modified Grashof number
G_r Grashof number

H Magnetic field intensity (kg s^{-2} A^{-1})
$\bar{H}_x, \bar{H}_x$ Dimensionless magnetic field intensity
H_0 Fixed magnetic field intensity (kg s^{-2} A^{-1})
J Current density (A m^{-2})
m Hall parameter
M Hartman number
P_r Prandtl number
R Joule heating parameter
R_m Magnetic Reynolds number
S_c Schmidt number
t Time (s)
T Temperature (K)
T_w Hot fluid temperature (k)
T_∞ Free stream temperature (K)
i, j, k Unit vectors
u,v Velocity components (ms^{-1})
$\bar{u}, \bar{v}$ Dimensionless velocity
u_0 Plate velocity (ms^{-1})
x,z Cartesian coordinates (m)
$\bar{x}, \bar{z}$ Dimensionless coordinates

Greek Letters

p_e Electron pressure (Pa)
n_e Density of electron (kg m^{-3})
Ω Angular velocity (s^{-1})
g Gravitational acceleration (m s^{-2})
α Angle of inclination
θ Dimensionless temperature
β Volumetric expansion (K^{-1})
ρ Density of the fluid (kg m^{-3})
q Velocity vector field
μ_e Magnetic permeability (N A^2)
τ_e Collision time of electrons (s)
ω_e Electron cyclotron frequency
ϑ Kinematic viscosity (m^2. s^{-1})
σ Electrical conductivity (S m^{-1}).

REFERENCES

1. Dulal P., Babulal T. Influence of Hall current and thermal radiation on MHD convective heat and mass transfer in a rotating porous channel with chemical reaction. International Journal of Engineering Mathematics. 2013: Volume 2013, Article ID 367064, 1–13.

2. Tania S.K., M. A. Samad. Effects of radiation, heat generation and viscous dissipation on MHD free convection flow along a stretching sheet. Research Journal of Applied Sciences, Engineering and Technology. 2010: 2, 368–377.

3. Siva R. S., Ali J. C., Anjan K. S. Thermal-diffusion and diffusion- thermo effects on MHD natural convective flow through porous medium in a rotating system with ramped temperature, International Journal of Numerical Methods for Heat & Fluid Flow. 2017: 27 (11), 2541-2480.

4. Liu I.C. A note on heat and mass transfer for a hydro magnetic flow over a stretching sheet. International Communications in Heat and Mass Transfer. 2005: 32(8), 1075–1084.

5. Makinde O.D. Similarity solution of hydromagnetic heat and mass transfer over a vertical plate with a convective surface boundary condition. International Journal of Physical Sciences. 2010: 5(6), 700–710.

6. Sengupta S., Shadap D. MHD dissipative fluid past a stretching sheet in the presence of Soret effect with Newtonian convective heat and mass conditions. Heat Transfer - Asian Research. 2018: 48(2), 1-14.

7. Seini Y.I, Makinde O.D. MHD boundary layer due to exponentially stretching surface with radiation and chemical reaction," Mathematical Problems in Engineering. 2013: 2013, 1-7.

8. Mahmud A., Mohammad R. MHD fluid flow of an incompressible electrically conducting fluid along a semi-infinite vertical porous plate under strong transverse magnetic field with rotation, Proceedings of the 8th BSME International Conference on thermal Engineering, Dhaka, Bangladesh, December, 2019.

9. Seth G.S., Nandkeolyar R. MHD couette flow in a rotating system in the presence of an inclined magnetic field. Applied Mathematical Sciences. 2009: 3, 2919 -2932.

10. Kinyanjui M.N, Emmah M., Kwanza J.K. Hydromagnetic turbulent flow of a rotating system past a semi-infinite plate with Hall current. International Journal of Pure and Applied mathematics. 2012: 79, 97-119.

11. Shamshuddin S. U, Kh.an O., B´eg A., B´eg T.A. Hall current, viscous and Joule heating effects on steady radiative 2-D magneto-power-law polymer dynamics from an exponentially stretching sheet with power-law slip velocity: A numerical study. Thermal Science and Engineering Progress, 2020: 1-13.

12. Nandkeolyar R., Das M. Sibanda P. Exact solutions of unsteady MHD free convection in a heat absorbing fluid flow past a flat plate with ramped wall temperature. Boundary value problem. 2013: 203, 1-16.

13. Seth G.S., Nandkeolyar R., Ansari M.S. Hartmann flow in a rotating system in the presence of inclined magnetic field with Hall effects. Tamkang J. Sci. Eng. 2010: 13, (3), 243-252.

14. Ahmed N., Sarmah H.K., Kalita D. Thermal diffusion effect on a three-dimensional MHD free convection with mass transfer flow from a porous vertical plate. Lat. Am. Appl. Res. 2011: 41, 165-176.

15. Eldabe N.T.M., Elbashbeshy E.A., Elsayed M.A. et al. Unsteady motion of MHD viscous incompressible fluid with heat and mass transfer through porous medium near a moving vertical plate. Int. J. Energy Technol. 2011: 3, 1-11.

16. Sharma G.K, Kumar L.K., Singh N. K. Unsteady Flow through Porous Media Past on Moving Vertical Plate with Variable Temperature in the Presence of Inclined Magnetic Field. (IJITR) international journal of innovative technology and research. 2016: 4(2), 2784-2788.

17. Prasad K.V., Vajravelu K., Vaidya H. Hall Effect on MHD flow and heat transfer over a stretching sheet with variable thickness. International Journal for Computational Methods in Engineering Science and Mechanics: 2016: 17(4), 288–297.

18. Maswai R.C., Kinyanjui M.N., Kwanza J.K. MHD turbulent flow in presence of inclined magnetic field past a rotating semi-infinite plate. International Journal of Engineering Science and Innovation. 2015: 4 (2), 344-360.

19. Iva L., Hasan M.S., Paul S.K., Mondal R.N. MHD free convection heat and mass transfer flow over a vertical porous plate in a rotating system with hall current, heat source and suction. International journal of advances in applied mathematics and mechanics. 2018: 6(1), 49 – 64.

20. Ngesa J.O., Kennedy O.A., Jeconiah O.A., Mark E.M. Heat and Mass Transfer Past a Semi-Infinite Vertical Porous Plate in MHD free convective flow in Turbulent Boundary Layer. World Journal of Research and Review. 2018: 6(2), 45 – 63.

21. Biswas R., Mondal M., Shanchia K. et al. Explicit finite difference analysis of an unsteady magnetohydrodynamics heat and mass transfer micropolar fluid flow in the presence of radiation and chemical reaction through a vertical porous plate. Journal of nano fluids: 2019, 8, 1583-1591.

22. Reza-E-Rabbi Sk., Arifuzzaman S.M., Sarkar T. et al. Explicit finite difference analysis of an unsteady MHD flow of a chemically reacting Casson fluid past a stretching sheet with Brownian motion and thermophoresis effects. Journal of King Saud University – Science. 2020: 32(1).

23. Ahmmed S.F., Biswas R., Afikuzzaman M. Unsteady Magnetohydrodynamic Free Convection Flow of Nanofluid Through an Exponentially Accelerated Inclined Plate Embedded in a Porous Medium with Variable Thermal Conductivity in the Presence of Radiation. Journal of Nanofluids. 2018: 7, 891–901.

24. Bulinda V.M., Kang'ethe G.P., Kiogora P.R. Magnetohydrodynamics Free Convection Flow of Incompressible Fluids over Corrugated Vibrating Bottom Surface with Hall Currents and Heat and Mass Transfers. Journal of Applied Mathematics. 2020: Volume 2020, 1-10.

25. Giterere K., Kinyanjui M., Uppal S.M. MHD flow in porous media over a stretching surface in rotating system with heat and mass transfer. International Electronic Journal of Pure and Applied Mathematics. 2012: 4(1), 9–32.

26. Meyer R.C. On reducing aerodynamic heat-transfer rates by magnetohydrodynamic techniques. Journal of the Aerospace Sciences. 1958: 25(9), 561–566.

27. Muthiga S.N., Kinyanjui M.N., Kiogora P.R. A Hydro-Magnetic Fluid Flow past a Rotating Semi-infinite Vertical Plate in the Presence of Variable Inclined Magnetic Field. International Journal of Engineering Science and Innovative Technology (IJESIT). 2018: 7(3).

28. Rout B.R., Parida S.K., Panda S. MHD Heat and Mass Transfer of Chemical Reaction Fluid Flow over a Moving Vertical Plate in Presence of Heat Source with Convective Surface Boundary Condition. International journal of chemical engineering. 2013: Volume 2013, Article ID 296834.

29. Adem G.A. Analytic Treatment for Electrical MHD Non-Newtonian Fluid Flow over a Stretching Sheet through a Porous Medium. Advances in Mathematical Physics. 2020: 2020, Article ID 8879264, 14 pages.

30. **Chenna Kesavaiah DAMALA**, Venkateswarlu BHUMARAPU, Oluwole Daniel MAKINDE (2021): Radiative MHD Walter's Liquid-B Flow Past a Semi-Infinite Vertical Plate in the Presence of Viscous Dissipation with a Heat Source, ***Engineering Transactions***, Vol. 69(4), pp. 373–401,

31. G Rami Reddy , **D Chenna Kesavaiah** , Venkata Ramana Musala and G Bkaskara Reddy **(2021):** Hall Effect on MHD Flow of a Visco-Elastic Fluid through Porous Medium Over an Infinite Vertical Porous Plate with Heat Source, ***Indian Journal of Natural Sciences,*** Vol. 12 (68), pp. 34975-34987